





Regulation of protein secretion through chemical regulation of endoplasmic reticulum retention signal cleavage

Arne Praznik^{1,2}, Tina Fink¹, Nik Franko ¹, Jan Lonžarić¹, Mojca Benčina ^{1,3}, Nina Jerala^{1,4}, Tjaša Plaper^{1,2}, Samo Roškar ¹ & Roman Jerala ^{1,3}✉

Secreted proteins, such as hormones or cytokines, are key mediators in multicellular organisms. Response of protein secretion based on transcriptional control is rather slow, as it requires transcription, translation and transport from the endoplasmic reticulum (ER) to the plasma membrane via the conventional protein secretion (CPS) pathway. An alternative regulation to provide faster response would be valuable. Here we present two genetically encoded orthogonal regulatory secretion systems, which rely on the retention of pre-synthesized proteins on the ER membrane (membER, released by a cytosolic protease) or inside the ER lumen (lumER, released by an ER-luminal protease), respectively, and their release by the chemical signal-regulated proteolytic removal of an ER-retention signal, without triggering ER stress due to protein aggregates. Design of orthogonal chemically-regulated split proteases enables the combination of signals into logic functions. Its application was demonstrated on a chemically regulated therapeutic protein secretion and regulated membrane translocation of a chimeric antigen receptor (CAR) targeting cancer antigen. Regulation of the ER escape represents a platform for the design of fast-responsive and tightly-controlled modular and scalable protein secretion system for mammalian cells.

¹Department of Synthetic Biology and Immunology, National Institute of Chemistry, Ljubljana, Slovenia. ²Graduate Study of Biomedicine, University of Ljubljana, Ljubljana, Slovenia. ³ENFIST Centre of Excellence, Ljubljana, Slovenia. ⁴Faculty of Medicine, University of Ljubljana, Ljubljana, Slovenia. ✉email: roman.jerala@ki.si

Protein secretion is an important cellular mechanism to translocate soluble or membrane-bound proteins in order to respond to the changes in the cellular environment or signals from other cells, thus influencing a wide range of biological functions. Indeed, it has been estimated, that out of the ~25,000 full-length open-reading frames (ORF) on the human genome, ~11% code for secretory proteins, with a further 20% for transmembrane proteins¹. Regulated secretion of a protein of interest (POI) would offer a valuable tool for a diverse range of functions, such as hormonal release, homeostasis, immune defense, cytokinesis² and quorum sensing³, as well as advanced therapeutic applications^{4,5}. Several attempts have been made to control protein secretion, mostly by utilizing the established systems which rely on the control of gene expression^{6–9}. These systems, while effective at regulating the production of proteins, are rather slow since they regulate gene expression rather than protein trafficking.

The processes of transcription and translation initiated by these systems can require several hours before the POI is secreted to a functionally relevant concentration. Natural processes, which need to respond rapidly to changes in the environment, often rely on the secretion of preformed proteins, stored in intracellular compartments and secreted quickly from the specialized cells by the regulated trafficking systems. Examples of such systems include the release of neurotransmitters into the synaptic cleft¹⁰ and insulin secretion from β -cells in the pancreas triggered by the increased concentration of glucose¹¹. While the aforementioned cells contain specialized granules and machinery, capable of exporting proteins in response to a defined signal, most, if not all, eukaryotic cells possess the ability to secrete proteins from the cell through natural secretion pathways. The best characterized of these is the conventional protein secretion (CPS) pathway, where proteins pass through the endoplasmic reticulum, towards the Golgi apparatus (GA), the trans-GA, and subsequently to the plasma membrane². Early in their synthesis, an N-terminal or, alternatively, an internal signaling sequence on the newly forming protein marks the protein to be directed towards the ER lumen, where it passes through to GA in Coat-protein complex II (COPII)-coated vesicles^{12,13}.

However, not all proteins that enter the ER are secreted—some proteins exert their function inside the ER and thus need to be retained there or recycled between the ER and the post-ER compartments. These proteins are typically marked with specific peptide tags, which distinguishes them from the proteins destined for secretion. The retention signal is recognized by specific receptors present in the ER and cis-GA, which retrieve the protein from post-ER compartments and return them to the ER by a retrograde translocation in COPI-coated vesicles. Examples of such sequences in animals include the C-terminal sequence motif Lys-Asp-Glu-Leu (KDEL), which is recognized by the KDEL receptor (KDELRL) and is present on soluble secretory proteins, and the Lys-Lys-X-X sequence (KKXX, where X stands for any amino acid), which interacts with the recycling COPI protein complex and is often present at the cytosolic side of transmembrane proteins¹⁴. In principle, marking a POI with an N-terminal signaling sequence and the C-terminal retention signal could therefore load and localize a POI inside the ER. Removal of the retention signal could provide an alternative system for controlling protein secretion. We reasoned that an important advantage of such a system would be a faster response than that achieved by the induction of gene expression, relying instead on the pre-synthesized protein pool stored in the lumen of the ER. Proteolytic removal of the ER retention signal by a regulated protease could therefore transduce the signal into protein secretion. Several viral proteases from the *Potyviridae* family have been recently described and utilized as functionally inactive split proteins,

which regain their catalytic activity upon reconstitution, triggered by several signals¹⁵. Since the viral proteases have a highly specific target sequence, they do not interfere with other cellular processes and are therefore valuable tools in synthetic biology for the generation of artificial protein-processing systems based on post-translational modifications^{15,16}. Here, we developed two systems for the controlled release of pre-synthesized proteins localized in the ER-lumen of mammalian cells, by proteolytic removal of an ER-retention signal sequence, based on the chemically regulated reconstitution of split potyviral proteases. Such a system is completely genetically encoded and its activation is considerably faster than systems based on the transcriptional induction of protein synthesis, since it relies on the pre-synthesized pool of proteins. This platform does not require the accumulation of protein aggregates in the ER that could trigger an aggregated protein stress response¹⁷. Chemically regulated proteases enable combinations of multiple orthogonal signals into logic gates with secreted protein as an output. In addition to the secretion of selected proteins, such as hormones or cytokines the described system can also regulate translocation of proteins to the plasma membrane, as demonstrated here for the chimeric antigen receptor (CAR) T cells.

Results

Design of member and lumER secretion system. Two types of ER-localized and proteolysis-based protein secretion systems were designed, each featuring a different C-terminal retention signal; the first type, termed member, was designed for membrane-bound proteins retained in the ER by the addition of a transmembrane domain and a C-terminal KKXX sequence exposed to the cytosol (Fig. 1a). This system is modeled after naturally occurring membrane-bound proteins localized in the ER. Based on previous reports, we opted to use the Lys-Lys-Met-Pro (KKMP) and Lys-Lys-Tyr-Leu (KKYL) sequences in the member system, which were shown to be particularly potent Golgi- to-ER retrieval signals^{18,19}. A transmembrane domain, from the B-cell antigen receptor complex-associated protein beta chain (CD79B) was used to anchor the protein of interest to the ER membrane. A potyviral protease cleavage site was inserted between the transmembrane domain and the ER retention signal, allowing for the control of secretion by the removal of the retention signal through proteolytic cleavage by a cytosolic protease.

The second type of an inducible protein secretion system, termed lumER, was designed for soluble proteins retained inside the ER lumen through the addition of a KDEL retention signal at their C-terminus (Fig. 1a). Binding of the KDEL sequence by the KDELRL (and thus recycling the POI back to the ER) is pH sensitive, with maximal binding at pH below 6²⁰. The acidic pH 6.2 inside the cis-Golgi lumen initiates binding, while the more neutral pH 7.2–7.4 inside ER lumen^{21,22} releases the interaction between KDEL and KDELRL. KDELRL itself features a KKXX retention signal at its cytosol-facing C-terminus, which interacts with the COPI vesicle machinery, responsible for the retro-transport of COPI vesicles from cis-Golgi to the ER²³.

Both member and lumER constructs were equipped with a signal peptide from the human immunoglobulin kappa²⁴ at the N-terminus of the secretion constructs to ensure translocation of the protein into the ER during translation (sequences in Supplementary Tables 1–3). However, because the two retention systems work through different pathways, each of them required additional unique design considerations. For the member system, removal of the retention signal enables the membrane-bound protein to bypass the cis-Golgi retro-transport, but once the protein passes through the GA, the protein remains anchored

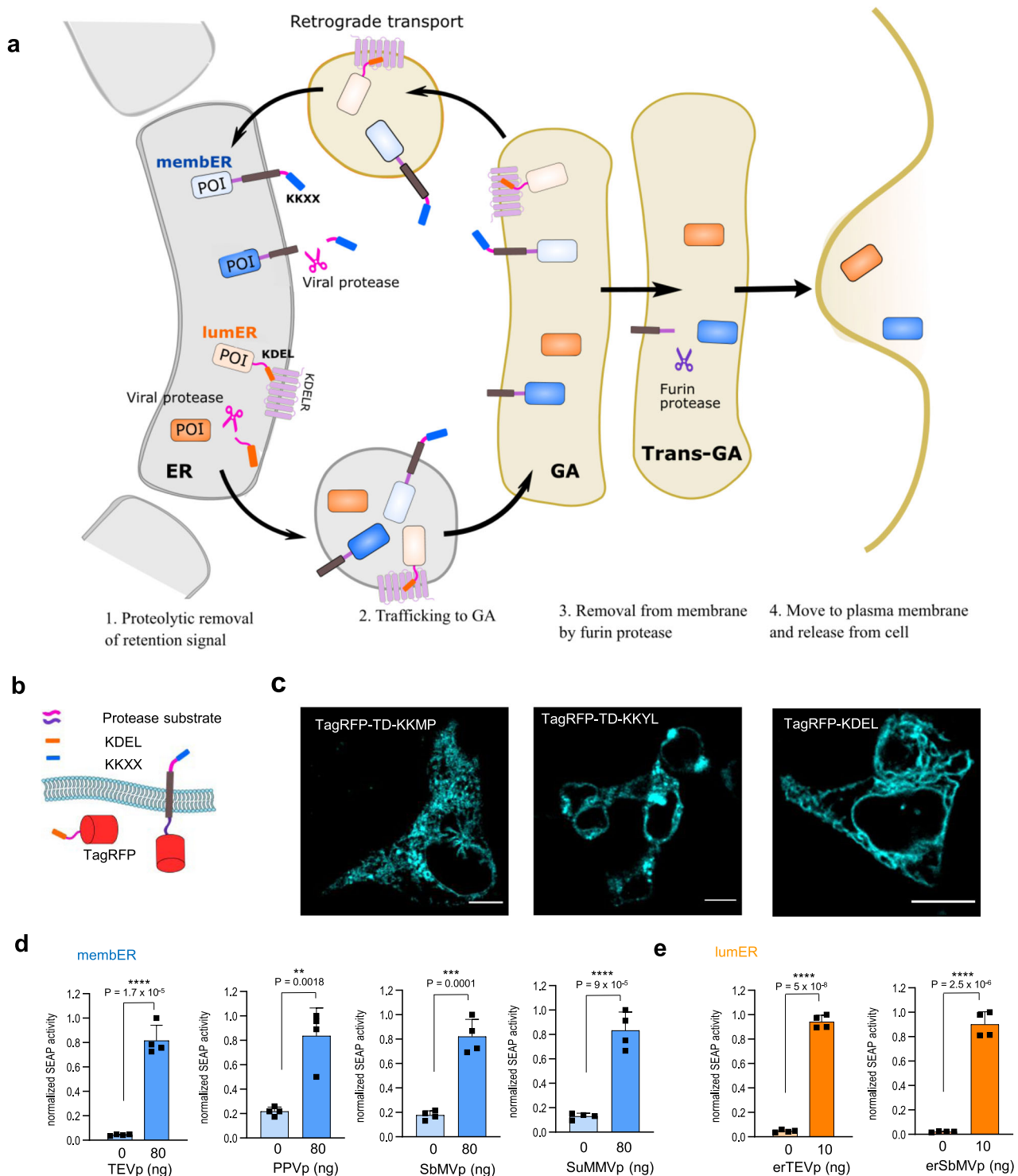


Fig. 1 Protease-inducible protein secretion by the membER and lumER systems. **a** Protease-triggered secretion of pre-synthesized protein from the ER is achieved by the cleavage of the C-terminal ER retention signal. A specific and orthogonal potyviral protease cleavage site was inserted between the protein of interest (POI) and the ER retention signal. Secretion is induced by the cytosolic protease (KKXX, membER system) or ER-localized protease (KDEL, lumER system). A furin protease (FURp) cleavage site (FURs) was inserted between the reporter and transmembrane domain to release the POI from the membrane for the membER system. **b** Design of the membER and lumER constructs featuring a TagRFP protein, which were used in microscopy imaging. **c** Imaging of TagRFP, featuring a transmembrane domain and a C-terminal KKMP, KKYL or KDEL sequence. Scale bar = 10 μ m. Images are representative of three independent experiments. **d** SEAP activity in cell supernatant was measured from cells transfected with membER constructs SEAP-FURs-TM-TEVs-KKYL, SEAP-FURs-TM-PPVs-KKYL, SEAP-FURs-TM-SbMVp-KKYL, or SEAP-FURs-TM-SuMMVp-KKYL and co-transfected with TEVp, PPVp, SbMVp, or SuMMVp, respectively. **e** SEAP activity in the cell media from cells transfected with lumER constructs SEAP-TEVs-KDEL or SEAP-SbMVp-KDEL was measured after the co-transfection of an ER-localized TEVp (erTEVp) or SbMVp (erSbMVp), respectively. Values are the mean of four cell cultures \pm s.d. An unpaired two-tailed *t* test (after equal variance was assessed with the F test assuming normal data distribution) was used for the statistical comparison of the data. Results are representative of three independent experiments. Source data are provided as a Source Data file.

into the cell membrane due to the transmembrane domain. To achieve the release of the POI from the plasma membrane once it had passed the GA and before reaching the plasma membrane, an additional furin protease (FURp) cleavage site (amino acid motif R-X-X-R²⁵) was inserted in the ER lumen-facing side of the target construct between the POI and the transmembrane domain. Since FURp is enriched in the GA²⁶, it cleaves the POI off the membrane, enabling its release upon the fusion of the secretory vesicles with the plasma membrane^{27–31}. The proteins presenting solvent-exposed R-X-X-R motif would be therefore cleaved on the way towards the plasma membrane.

On the other hand, the lumER secretion design relies on retention in the ER by the KDEL, which recognizes and binds the ER lumen-exposed C-terminal KDEL signal. For this reason, the lumER constructs do not need to be anchored to the ER-membrane for them to be retained in the ER and thus only require the N-terminal signal peptide and the C-terminal KDEL sequence, separated from the POI by a selected protease cleavage site (Abstract figure, Fig. 1a). However, the proteolytic processing in the lumER system occurs inside the ER lumen, thus requiring a protease which retains its location and activity within the secretory pathway. Additionally, this protease would need to be equipped with a signal sequence, for the transport into the ER, and a retention signal to halt its progression to the cell surface. We found a previously described ER-localized TEVp, termed erTEVp, appropriate for the execution of the proteolytic processing inside the ER lumen³² that could be regulated by a chemical signal. To expand the repertoire of functional proteases used in our secretion systems, we replaced the TEVs in the member system with a cleavage site of other orthogonal viral proteases from the *Potyviridae* family of viruses, namely plum pox virus protease (PPVp)³³, soybean mosaic virus protease (SbMVp)³⁴, and sunflower mild mosaic virus protease (SuMMVp)³⁵, which have been previously utilized in the SPOC system, the synthetic protease and coiled-coil-based signal-processing system¹⁵. In a similar fashion to the described erTEVp, an ER-localized SbMVp (erSbMVp) and PPVp (erPPVp) were designed to also feature an N-terminal signal sequence and C-terminal KDEL sequence for use with the lumER system.

Protease-dependent release of proteins from mammalian cells.

For visualization of trafficking of the member and lumER constructs within the cell, TagRFP³⁶ was fused to secretion constructs and expressed in HEK293T cells. The addition of a signaling sequence and a retention signal localized the constructs mostly in the ER (Fig. 1 b, c, Supplementary Figs. 1, 2a, b, c). For detection of proteins released into the cell media upon coexpression of an appropriate protease, reporter proteins secreted alkaline phosphatase (SEAP) and Gaussia luciferase (Gluc) were incorporated into the lumER and member systems. The expression of both lumER-SEAP and member-SEAP was verified by Western blot (Supplementary Fig. 2d, e). Since the implementation of KKYL retention signal produced less leakage compared to the KKMP (Fig. 1d, Supplementary Fig. 3a), we opted for the use of the former retention signal in the member system. We found that all four tested potyviral proteases were capable of inducing secretion when co-transfected with a member construct containing the appropriate substrate. However, TEVp provided the best fold increase of the secreted reporter into the media in the presence of the protease (Fig. 1d). Since secretion of the member system depends on FURp processing to release the protein from the plasma membrane, cells were co-transfected with a plasmid expressing the native FURp. A further increase in the amount of a secreted protein was observed when FURp was added, without

increasing protein secretion in the absence of a protease (Supplementary Fig. 3b). In summary, implementation of the member secretion system with 4 orthogonal and highly specific proteases was demonstrated.

lumER-based SEAP secretion is controlled by the proteolytic processing by an ER-localized protease. Reporter secretion was minimal in the absence of a potyviral protease, while the addition of erTEVp led to the 20-fold increased release of SEAP into the media (Fig. 1e). Similarly, we tested PPVp and SbMVp on the lumER system, by replacing the TEVs with PPVs and SbMVs, and directing the two proteases into the ER lumen through inclusion of a signal peptide and a KDEL sequence. Coexpression of an ER-targeted PPVp however did not lead to the release of SEAP into the cell medium (Supplementary Fig. 3c). A large proportion of proteins traversing through ER and GA is processed by a diverse array of post-translational modifications, most notably glycosylation by ER- and GA-resident glycosyltransferases, which can modify proteins³⁷. Glycosylation might decrease or altogether abolish the activity of a protein, depending on its position within the protein. Indeed, TEVp required mutations at two sites to prevent glycosylation and maintain its activity inside the ER lumen³². An N-glycosylation site prediction tool NetNGlyc 1.0 Server (<http://www.cbs.dtu.dk/services/NetNGlyc/>) revealed two potential glycosylation sites in PPVp (N23, N173), potentially explaining the observed lack of activity of this protease in the ER. After changing the two amino acid residues (N23Q, T173G) at positions corresponding to erTEVp, small increase of secretion was observed (Supplementary Fig. 3d). ER-targeted SbMVp, on the other hand, was able to induce strong secretion of SEAP (Fig. 1e), demonstrating here for the first time the activity and retention of SbMVp in the ER, therefore providing an additional orthogonal regulator of protein secretion.

The addition of several TEVs between the retention signal and transmembrane domain increased the secretion of SEAP after the addition of TEVp (Supplementary Fig. 3e), likely due to an increased accessibility of the substrate and increased distance between the ER membrane and the retention signal³⁸. Increasing the amount of TEVp in combination with the member constructs led to the increased secretion of SEAP (Supplementary Fig. 3f). On the other hand, increasing the amount of the ER-localized protease in the lumER system above a certain threshold led to a decreased secretion of SEAP (Supplementary Fig. 3g). We reasoned that this might be due to the competitive binding of the erTEVp to the KDEL, which also features a KDEL retention sequence on its C-terminus, and could lower the capacity of the retrograde transport. This was indeed confirmed by rescuing reporter secretion by the ectopic expression of the KDELRL1, which led to an almost 2-fold increase of the amount of secreted SEAP triggered by the erTEVp (Supplementary Fig. 3h).

Kinetics of the member and lumER secretion systems. We next aimed to regulate secretion using chemically inducible proteases. For this purpose, the FKBP/FRB and ABI/PYL1 heterodimerization domain pairs were used as chemically induced dimerization (CID) systems regulated by rapamycin³⁹ and abscisic acid (ABA)⁴⁰, respectively. Both CID systems were used to reconstitute split fragments of the four aforementioned potyviral proteases, which regained their activity upon heterodimerization. For use in the ER lumen, we designed pairs of split protease fragments of erTEVp, a signal sequence and a KDEL retention signal, fused to CID domains. The resulting pairs were termed er-rapa-TEVp and er-aba-TEVp (Fig. 2a). HEK293T cells expressing the member secretion system with SEAP as the POI and FKBP-cTEVp/FRB-nTEVp (rapa-TEVp) or ABI-cTEVp/PYL1-nTEVp (aba-TEVp) as the inducible split protease, secreted SEAP when stimulated with rapamycin or ABA,

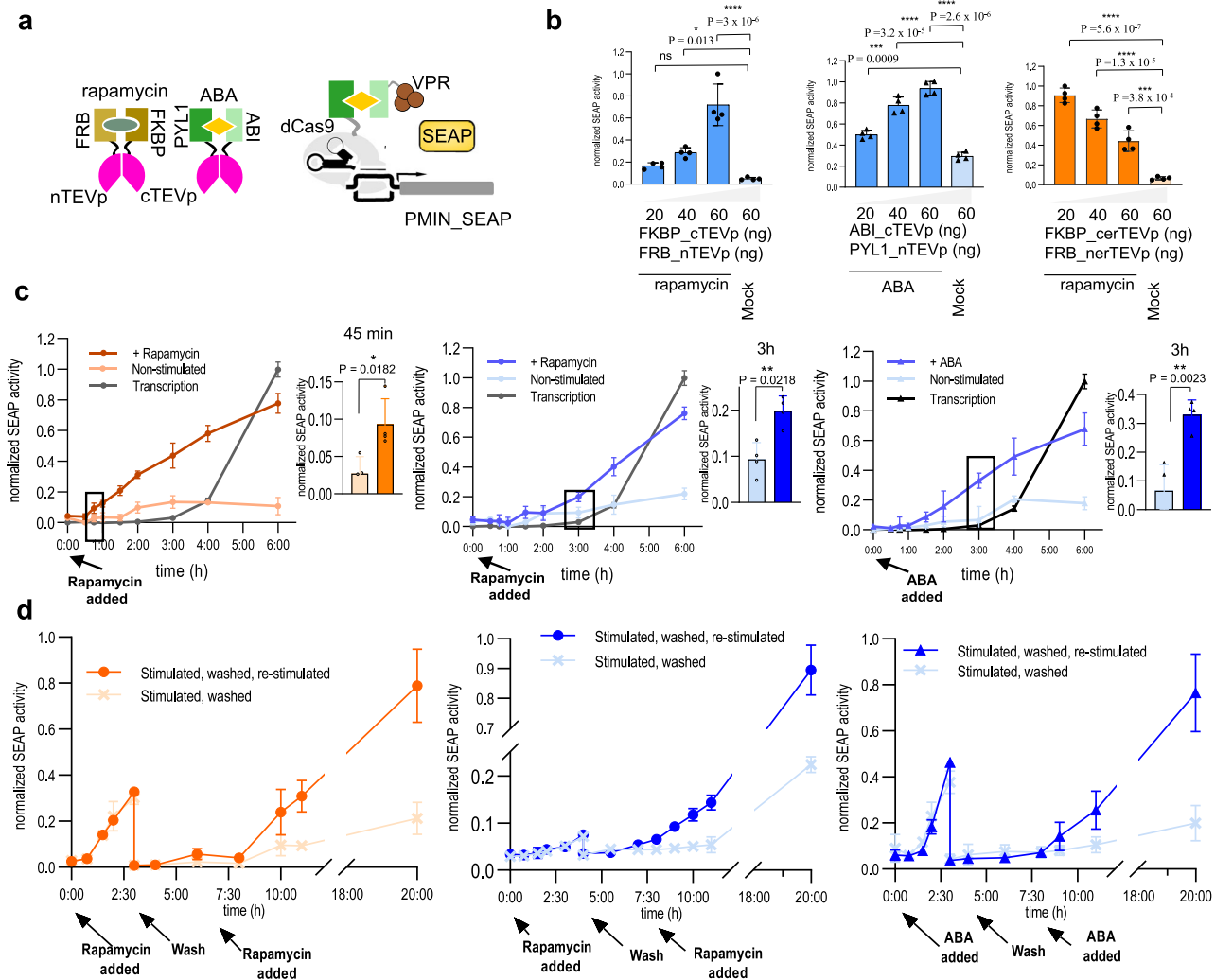


Fig. 2 Inducibility and kinetics of protein secretion. **a** For the inducible protein secretion, split protease fragments were fused to the chemically inducible dimerization partners FKBP/FRB or ABI/PYL1. For localization within the ER lumen, the inducible proteases were equipped with an N-terminal signal sequence and a C-terminal KDEL. Reconstitution of the protease was achieved by the addition of rapamycin in the case of FKBP/FRB or ABA in the case of ABI/PYL1. To compare the kinetics of secretion of our pre-synthesized proteins with secretion initiated by SEAP expression, a dCas9-FKBP/FRB-VPR or dCas9-ABI/PYL1-VPR system with an addition of an sgRNA targeting a minimal promoter upstream of the SEAP reporter gene, was utilized, where expression of SEAP was initiated by either rapamycin or ABA, respectively. **b** Cells were transfected with SEAP-TEVs-KDEL and FKBP-cerTEVp/FRB-nerTEVp (er-rapa-TEVp; orange), SEAP-FURs-TM-TEVs-KKYL and FKBP-cTEVp/FRB-nTEVp (rapa-TEVp) or ABI-cTEV/PYL-nTEV (aba-TEVp) (blue). SEAP activity was measured in the media after 20 h after the addition of rapamycin or ABA. **c** Secretion of SEAP was monitored after the addition of rapamycin for the lumER (orange) and rapamycin or ABA for the membER (blue) system and compared to the expression-driven secretion. **d** Secretion was induced by the addition of rapamycin or ABA. After 4 h, the medium was removed, the cells were washed and supplementary medium was added. After an additional 3 h cells were restimulated. SEAP activity in the media was measured continuously. Values are the mean of four cell culture experiments \pm s.d. Significance was tested by an unpaired two-tailed t test or one-way analysis of variance (ANOVA) with Dunnett’s comparison (values of confidence intervals, degrees of freedom, F and P are indicated). Results are representative of three (**b, c**) and two (**d**) independent experiments. * $P < 0.05$, ** $P < 0.01$, *** $P < 0.001$, **** $P < 0.0001$. Source data are provided as a Source Data file.

respectively (Fig. 2b). As with single-chain proteases, the KKYL retention signal resulted in higher fold of induction than KKMP (Fig. 2b, Supplementary Fig. 4).

Chemical stimulation of cells expressing er-rapa-TEV and the lumER secretion system resulted in an inducible secretion of SEAP (Fig. 2b). Similar to the single chain protease, higher amount of er-rapa-TEV resulted in a decreased amount of secreted SEAP after stimulation with rapamycin (Supplementary Fig. 5a), which can be attributed to the competition with the KDEL receptor. In the case of er-aba-TEV heterodimerization domains within the ER, no secretion was detected for ABA stimulation (Supplementary Fig. 5b). The N-glycosylation site prediction tool indicated several potential glycosylation sites on

both ABI and PYL1 heterodimerization domains (ABI: N292; PYL1: N66, N90), which likely hindered its function in the ER.

Rapamycin, on the other hand, was able to induce secretion already at picomolar concentrations and reached a plateau at approximately 25 nM with the membER system and 10 nM with the lumER system, while ABA was able to induce secretion in the membER system at nanomolar concentrations and reached a plateau at approximately 0.5 mM concentration (Supplementary Fig. 6). Taken together, both systems were able to elicit a concentration-dependent secretion of POI, however ABA-inducible secretion functioned only for the membER system.

To monitor the secretion kinetics, cells harboring constructs for secretion systems and split chemically inducible TEVp were

stimulated either with rapamycin or ABA and cell medium was harvested at designated time points. To directly compare the kinetics of a chemically regulated secretion system with a chemically regulated transcriptional activation system, we placed the expression of SEAP under a minimal promoter that was regulated by an inducible CRISPR-based transcription factor. A dCas9 protein fused to FKBP or ABI (dCas9:FKBP and dCas9:ABI) was brought into the proximity of the promoter by an sgRNA targeting the minimal promoter sequence. Transcription was initiated by the addition of rapamycin- or ABA-inducing heterodimerization of the dCas9 fusion with the transcription activator domain VPR fused to the complementary CID protein (FRB:VPR or PYL1:VPR, Fig. 2a). Secretion kinetics for memberER, lumER and the transcriptional activation-based systems were measured and compared at varying concentrations of the chemical inducers (Supplementary Fig. 7). While the proteolysis-based secretion systems were able to induce secretion in less than 1 h, the transcriptional activation-based secretion was only observed after several hours. The lumER system was able to induce secretion with faster kinetics than the memberER system; in the former a statistically significant increased amount of SEAP in the cell media compared to non-stimulated cells was observed at 45 min (Fig. 2c). While the additional co-transfection of FURp with the memberER system demonstrated increased secretion after the extended time (Supplementary Fig. 3b), it did not significantly increase the secretion in the first 4 h (Supplementary Fig. 8).

We next tested the ability of both secretion systems for multiple stimulations. After induction with either rapamycin or ABA, cell media were sampled for up to 3–4 h, whereafter the cells were washed and fresh media were supplemented. SEAP concentrations continued to remain low in the media up until 4 h after washing, after which cells were restimulated and a repeated secretion of SEAP was observed in stimulated cells, with minor leakage from the unstimulated cells even after 20 h (Fig. 2d), suggesting that both systems could be activated with multiple pulses. We cannot however exclude the possibility that the first rapamycin stimulus did not deplete all synthesized protein from the ER leaving the second pulse with no more protein to release. Therefore, we next determined how long it takes to release the total amount of the ER-localized protein pool from the cell after the induction of secretion. Since the constitutive expression of our constructs is continuously replenishing the ER with the new biosynthesis of POI, we aimed to halt the transport of newly formed protein into the ER lumen, so that only the pre-synthesized ER protein pool could be secreted. Cells were treated with Eeyarestatin I (Sigma-Aldrich, E1286), a potent inhibitor of Sec61-mediated protein translocation into the endoplasmic reticulum, which has been shown to inhibit secretion of cellular proteins at the ER-resident ribosomal biosynthesis step⁴¹. Media were harvested after induction of secretion with rapamycin. We observed that the majority of the available SEAP was secreted within 6–7 h after stimulation for both memberER and lumER system (Supplementary Fig. 9).

The intracellular trafficking of memberER and lumER proteins within the cell was monitored under the fluorescence microscope, by the inclusion of a super-folder GFP (sfGFP), split into two segments between the 10th (GFP1-10) and 11th β -strand (GFP11), which have been previously shown to allow for a high resolution imaging within cells⁴². GFP1-10 was fused to the memberER (SS-GFP1-10-FURs-TD-TEVs-KKYL) and lumER (SS-GFP1-10-TEVs-KDEL) secretion systems, while seven tandem repeats of GFP11 (GFP11x7) were fused to the human Fas receptor transmembrane domain. The trafficking of the ER-localized construct to GA and further to the plasma membrane could be visualized by the reconstitution of the split sfGFP when they were localized in the same cellular compartment (Supplementary Figs. 10a, 11a). Since the GFP11x7 fragment, once produced, needs to pass the ER to

reach GA and the plasma membrane, the fluorescence could be already observable in the ER (Supplementary Figs. 10b, 11b). Both the lumER and memberER systems retained the reconstituted protein within the ER when no protease was added. Coexpression of TEVp and erTEVp led to the appearance of a fluorescent signal at the plasma membrane (Supplementary Figs. 10b, 11b). The reconstitution of a split TEVp and split erTEVp similarly led to the accumulation of the split GFP fragments at the plasma membrane after 3 h (Supplementary Figs. 10c, 11c). When visualizing a group of cells, a noticeable increase in fluorescence was observed in the GA in less than 15 min after stimulation with rapamycin, while the signal at the plasma membrane was observed after 1 h (Fig. 3).

Since the two systems are based on differently localized proteases and different recycling signals it is likely that they could be regulated independently. Orthogonality of the two secretion systems was tested by co-transfecting both the lumER and memberER systems simultaneously. For the memberER system a SEAP reporter was used, while the lumER was fused to a Gluc reporter (Fig. 4a). Cells expressing both systems were co-transfected with TEVp, erTEVp or both proteases and measured Gluc and SEAP activity in the media. Each system elicited secretion only in the presence of the appropriate protease (Fig. 4b). Similarly, we managed to elicit the selected secretion by co-transfecting a cytosolic aba-TEVp and ER-localized er-aba-TEVp (Fig. 4c) and inducing secretion by the addition of either ABA or rapamycin (Fig. 4d).

Construction of an input signal-processing module to regulate protein secretion via the memberER and lumER systems.

The ability to regulate the removal of the retention sequence with several chemical or biological signals would allow for a stringent control over protein secretion, as well as allow the system to be controllable by different combinations of external but also internal signals. While KKYL or KDEL is required at the C-terminus of the protein to be retained within the ER, only a single retention signal can be present on each protein, making it difficult to design a construct responding to a combination of two inputs, with the exception of an OR gate. We therefore employed the previously described SPOC system¹⁵, based on split proteases and combinations of coiled-coil peptides, which is able to process two-input signals according to Boolean logic operations and produce an output in the form of a reconstituted pottyr viral protease activity¹⁵. The reconstituted pottyr viral protease could therefore be further used to regulate protein secretion. The principle of SPOC logical circuits used in this study is described in Supplementary Fig. 12. We employed the constructs to demonstrate an A implies B function, activated by the presence of one signal and the absence of the other one (Fig. 5a), as well as an AND function, activated by the presence of both signals using memberER secretion system (Fig. 5b), both with excellent difference between the active and inactive output state. However, any two- or multiple input Boolean logic could be implemented in principle.

Optimization of each protease to retain its activity in the ER for lumER system would likely need to be accomplished by the introduction of appropriate mutations in the proteases, as demonstrated in this study. More importantly however, transferring the components of SPOC into the ER might increase leakage of the system due to the saturation of the recycling machinery. We therefore employed an alternative strategy to adapt SPOC to lumER and designed a system that allows retention of proteins in the ER and their release upon signal processing of two-input signals. We appended the KDEL sequence to an ER-localized designed coiled-coil forming P3 peptide via a TEVp cleavage site (P3-TEVs-KDEL), which interacts with its complementary

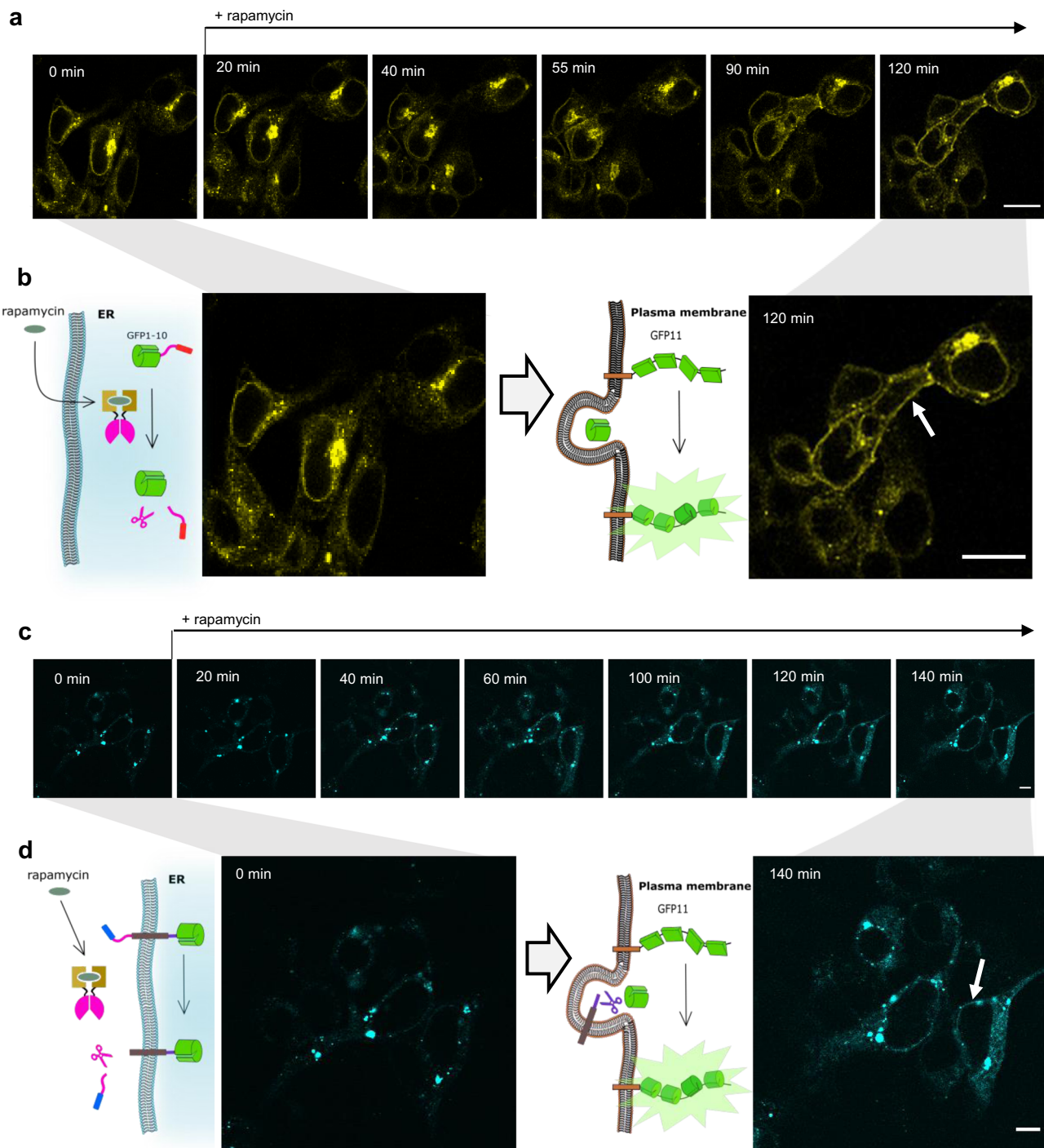


Fig. 3 Single cell visualization of protein trafficking in the lumER and member system. **a** GFP signal was visualized on the same group of cells over a period of 2 h. **b** Close up of cells before the addition of rapamycin and of 2 h after the addition of rapamycin. The signal begins to appear at the plasma membrane (white arrow) after ~60 min. **c** GFP signal was visualized on the same group of cells over a period of 140 min. The signal begins to appear at the plasma membrane (white arrow) after ~110 min. **d** Close up of cells before the addition of rapamycin and 140 min after the addition of rapamycin with an arrow indicating localization at plasma membrane. Scale bar = 10 μ m. Images are representative of three independent experiments. Source data are provided as a Source Data file.

peptide P4, located on our POI (SEAP-P4). The interaction of P3/P4 coiled-coil pair was capable of retaining SEAP within the ER when the KDEL sequence was present only on one of the two interacting constructs (Supplementary Fig. 13a). In this system, cleavage with TEVp resulted in the release of a POI. To perform an AND function in the lumER system, an additional KDEL

sequence was fused to the protein of interest with SBMVs inserted between P4 and KDEL (SEAP-P4-SbMVp-KDEL) (Supplementary Fig. 13b). This resulted in induction of secretion only when both erTEVp and erSbMVp are present (Fig. 5c).

To further control secretion, we aimed at establishing a simplified version of an AND logic function to function as

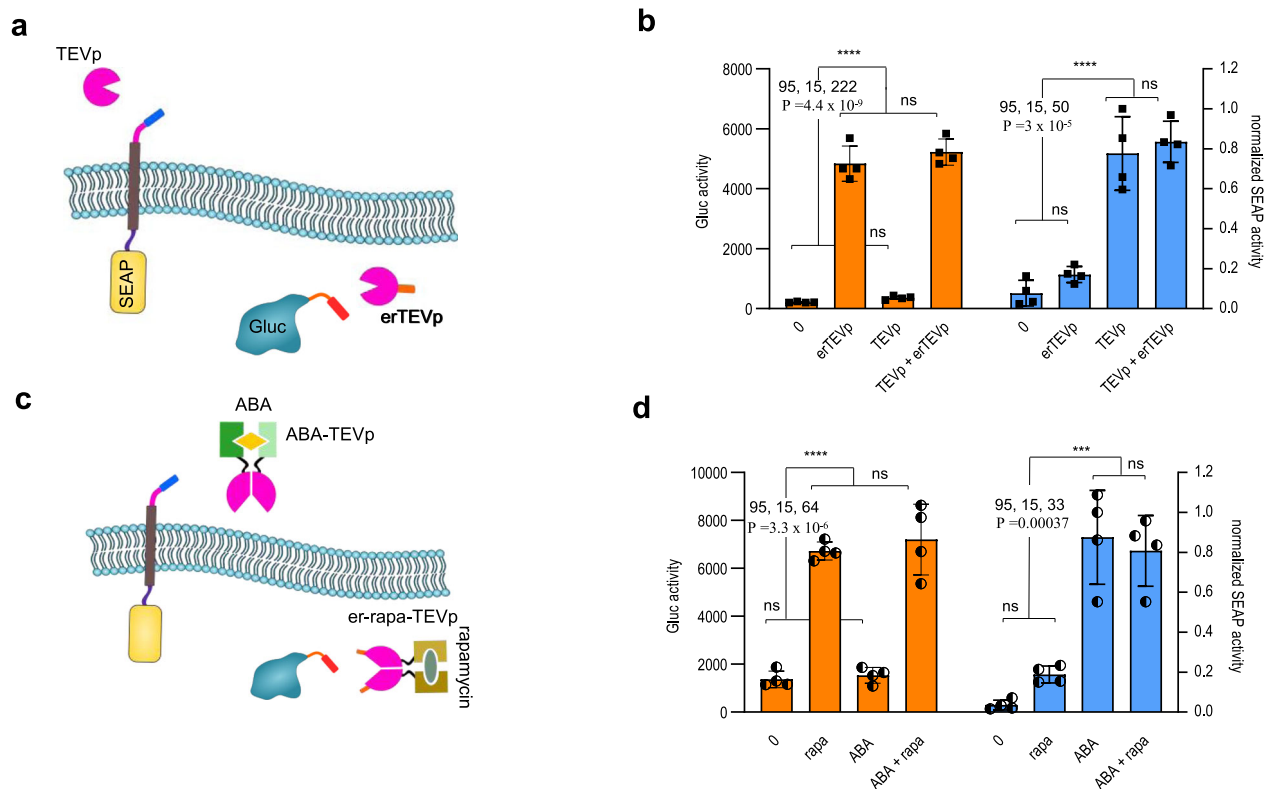


Fig. 4 Orthogonality of the lumER and membER system. **a** Cells were co-transfected with memberER system, featuring SEAP as a reporter, and lumER system, featuring a Gluc reporter. **b** Gluc (orange) and SEAP (blue) activity was measured in the media after the addition of TEVp and erTEVp. **c** Design of the inducible and orthogonal system. aba-TEVp and er-rapa-TEVp were co-transfected with the memberER-SEAP and lumER-Gluc constructs. **d** the systems were tested with inducible proteases. aba-TEVp was used for secretion with the memberER (blue) and er-rapa-TEVp was used for the lumER system (orange). Values are the mean of four cell cultures \pm s.d. and are representative of two independent experiments. Significance was tested by one-way analysis of variance (ANOVA) with Tukey's comparison between indicated states (values of confidence intervals, degrees of freedom, F and P are indicated). * $P < 0.05$, ** $P < 0.01$, *** $P < 0.001$, **** $P < 0.0001$. Source data are provided as a Source Data file.

an OFF switch, which was intended to halt secretion, at some selected delay after it had been initiated. For this purpose, we inserted PPVs between the heterodimerization domains and the split TEVp fragments (FKBP-PPVs-cTEVs, FRB-PPVs-nTEVp). The addition of PPVp cleaves off the split protease fragments from the heterodimerization domains, preventing their reconstitution and, consequently, secretion (Supplementary Fig. 14). To make the OFF switch inducible, ABA CID heterodimerization domains were used to control the assembly of PPVp (ABI-cPPVp/PYL1-nPPVp) (Fig. 5d). Cells which had been stimulated with rapamycin and were subsequently stimulated with ABA, demonstrated a decreased secretion of SEAP into the media compared to cells only stimulated with rapamycin (Fig. 5d).

Control of therapeutically relevant protein trafficking using lumER and membER systems. Finally, we applied our secretion system to therapeutically relevant proteins, where fast release upon stimulation is important. Diabetes mellitus affects millions of people worldwide and is characterized by depletion or exhaustion of insulin-producing β -cells in the pancreas⁴³. Insulin is normally secreted from specialized granules inside of β -cells and is tuned to be released within minutes to hours after the rise of blood glucose level⁴⁴. Engineered systems have been previously designed to trigger the release of insulin or GLP-1, which however exhibited a response time of several hours⁶. A system for the release of pre-synthesized proteins relied previously on protein aggregation inside the ER lumen³¹. This platform may however lead to increased ER stress, which could result in apoptosis⁴⁵. In

comparison to previously described systems based on conditional protein aggregates in the ER³¹, the lumER and membER system prevented activation of ER stress-characteristic XBP1 and decreased cell viability, even when overexpressed (Supplementary Fig. 15), demonstrating its advantage to ER stress-sensitive cells. We used a design of human insulin adapted for protease processing and secretion through the conventional secretion pathway⁴⁶. This was achieved by modification of the insulin sequence to feature two FURs surrounding the C-peptide, which could be processed to a mature insulin by FURp. The preproinsulin sequence was appended to the lumER secretion system (Fig. 6a) and combined with the er-rapa-TEV. Human insulin levels secreted by HEK293T cells were quantified by measuring the amount of secreted C-peptide upon rapamycin stimulation. Alternatively, a reporter system was designed, which substituted the C-peptide of a preproinsulin with a short secretory Gaussia luciferase, which has been previously used as a surrogate reporter of insulin secretion^{47,48} (Supplementary Fig. 16). Elevated C-peptide levels were detected in cell media as early as 30 min after the addition of rapamycin (Fig. 6b). The presence of a C-peptide in cell media in the case of the lumER system was detected within 45 min, in contrast to several hours, in the case of a system based on the transcriptional induction of insulin expression by the addition of rapamycin (Fig. 6b). Using a similar strategy, the membER system was demonstrated to control the release of the anti-inflammatory cytokine interleukin 10 (IL-10), a potential therapeutic protein for several therapeutic indications⁴⁹. Increased levels of IL-10 were observed rapidly after induction of secretion with rapamycin (Fig. 6c).

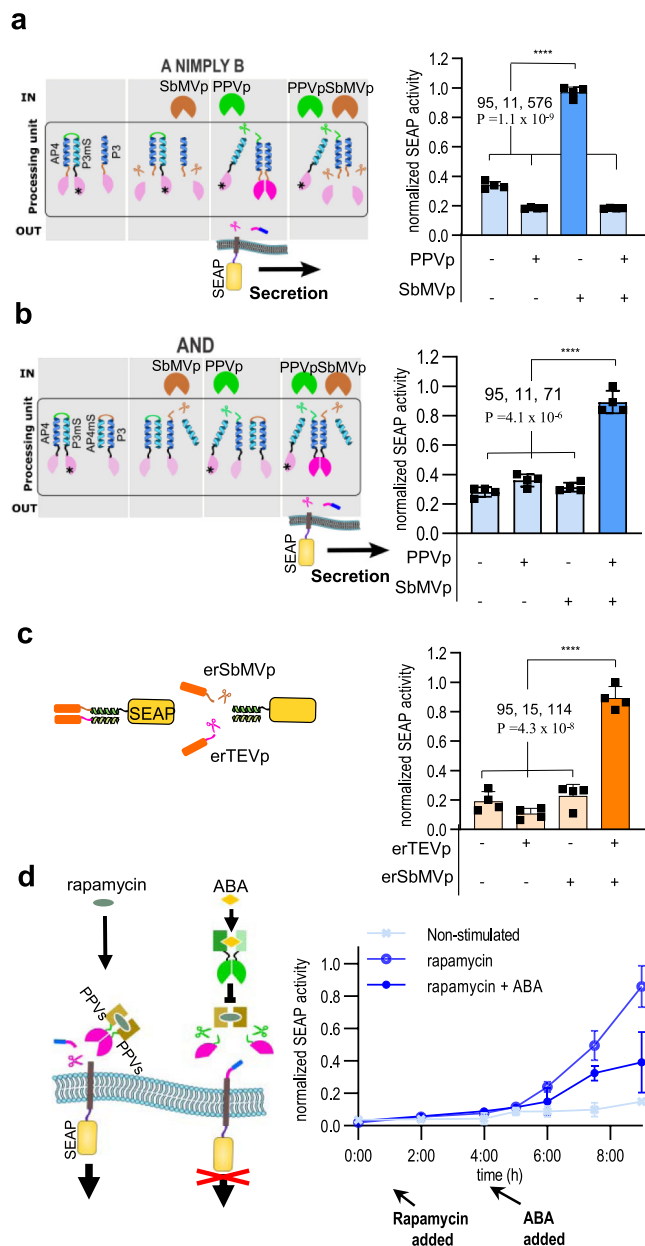


Fig. 5 Modular combinations and two-input signal-processing capacity of protein secretion systems. **a** A two-input Boolean logic processing system - SPOC, previously described by Fink *et al.*, was used to control the reconstitution of a split TEVp and regulate secretion through the removal of KKYL. The input proteases SbMVp and PPVp produced the output according to A nimply B logical function and **(b)**, AND logical function. For the KDEL system, SEAP was retained inside the ER by the addition of a C-terminal KDEL sequence, as well as the retention of the construct through the interaction of the P3/P4 coiled coils, where P3 also featured SbMVs and a KDEL sequence. Secretion was induced by the addition of erTEVp and erSbMVp. **c** To establish an AND function for the lumER system, P3-TEVs-KDEL was co-transfected and localized inside the ER with SEAP-P4-SbMVs-KDEL. Apart from the KDEL sequence (orange) present on the same protein, SEAP was retained inside of the ER through the P3/P4 coiled-coil interaction. To facilitate the secretion of SEAP, both erSbMVp and erTEVp have to be present, in order to remove the two retention signals. **d** Implementation of a protein secretion OFF switch. Rapamycin is used to reconstitute a split TEVp, which further drives secretion of the membER secretion construct. By inserting a PPVp cleavage site (PPVs) between the dimerization domain and protease fragment, the reconstitution of TEVp can be inhibited with an ABA-inducible split PPVp. Cells were stimulated with rapamycin to induce secretion. After 3 h ABA was added and cell media were harvested continuously for 6 h. Values are the mean of three **(d)** or four cell **(a, b, c)** cultures \pm s.d. and are representative of two independent experiments. Significance was tested by one-way analysis of variance (ANOVA) with Dunnett's comparison between indicated ON and OFF states (values of confidence intervals, degrees of freedom, F and P are indicated). Source data are provided as a Source Data file.

to target B-cells presenting CD19 (Fig. 6d, e; Supplementary Fig. 17), which could be used to license the therapeutic response to a level comparable to the clinically used CAR construct design.

Discussion

Several biological processes require a response within minutes to hours, in order to elicit a physiologically relevant response, which could not be achieved using a transcriptional control. Examples of processes that require fast response include the release of hormones depending on the physiological conditions, such as insulin after a meal, release of pro- and anti-inflammatory cytokines, anti-microbial or anti-viral peptides and others⁵²⁻⁵⁸. Therefore the development of accelerated protein secretion systems based on genetically encoded components offers an attractive venue for delivering biotherapeutic agents in situ in a physiologically relevant timeframe⁴. Natural protein secretion systems that are able to respond rapidly to input signals, often achieve this in specialized cells by forming storage granules, containing pre-synthesized protein, which are positioned close to the plasma membrane and fuse with the plasma membrane upon signal detection. Biosynthesis of secretory granules in specialized cells involves tens of genes and is still a relatively unknown process⁵⁹. Additionally, those specialized cells may be unwantedly triggered by external signals⁶⁰. Alternatively, accelerated kinetics of selected protein release in nonspecialized cells based on the principle of storing pre-synthesized proteins and releasing them upon stimulation is an attractive approach to engineer systems for protein release or translocation to the plasma membrane. This could have an important advantage for cases where a rapid response is required such as e.g. for hormone secretion or the control of activation of immune cells to rapidly prevent escalation into an uncontrolled excessive response, which we demonstrated on the examples of protein secretion and translocation to the plasma membrane. While external chemical signals were used in this study to exert external control, a relevant biological process or pathogen-specific protease might be used as well as an independent signal.

In addition to secretion of soluble proteins, translocation of membrane-associated proteins to the plasma membrane may be useful for a therapeutic application. Chimeric antigen receptors are used to armor T cells against cancer cells presenting specific membrane markers, such as e.g. CD19 for B-cell leukemias and lymphomas. Regulation of CAR T cell responsiveness is desired, as the excessive activation of engineered T cells may lead to often fatal cytokine release syndrome. Apart from the strategy using a kill switch^{50,51}, which permanently eliminates therapeutic cells, regulation of the activity of CARs² represents a better alternative but its response may be slow. We proposed here to regulate translocation of CARs to the plasma membrane using a chemically regulated translocation system. In this case CARs are restricted within the cell until the signal triggers their rapid translocation to the plasma membrane, where they can engage target cells and trigger cell activation. CARs were engineered to comprise the ER retention signal that could be cleaved off by the chemically regulated protease. The system was demonstrated to regulate translocation of CARs to the plasma membrane, resulting in chemical regulation of the response of CAR T cells

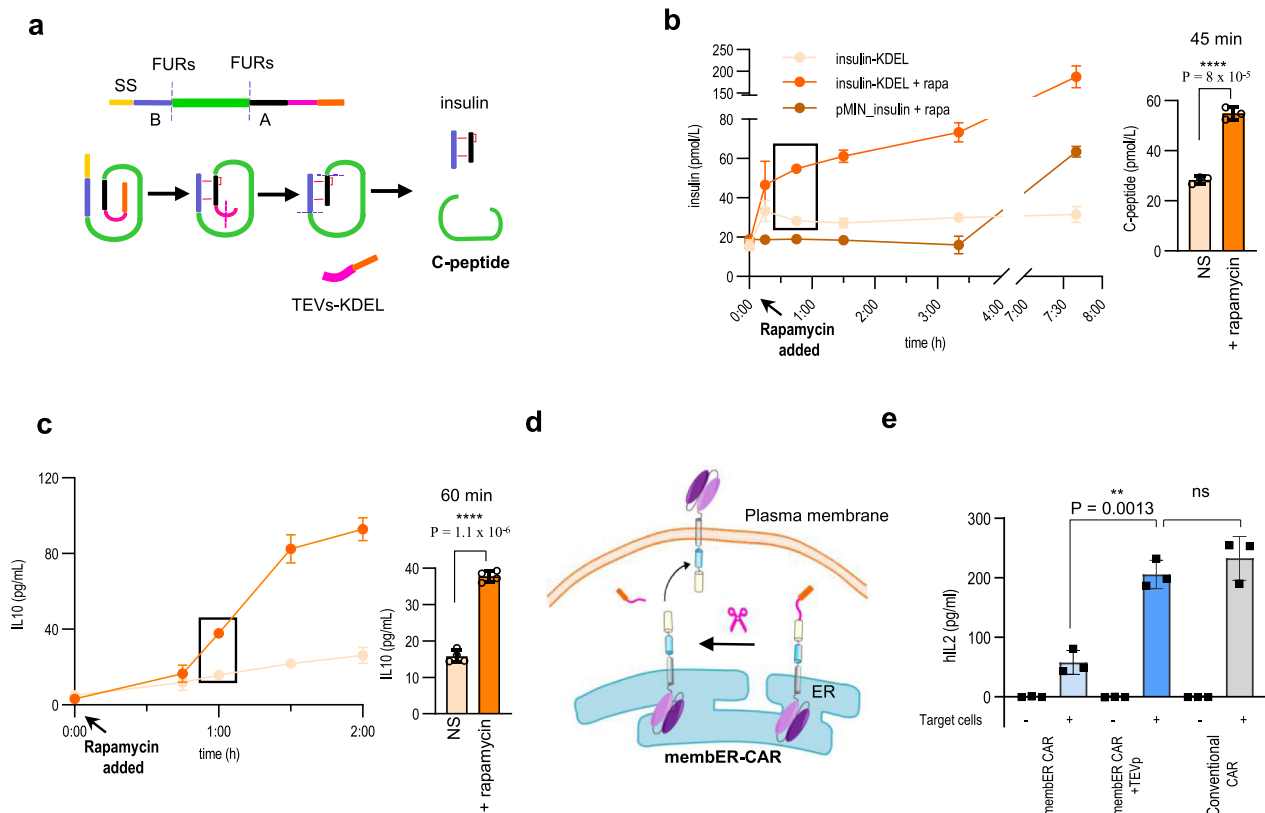


Fig. 6 Inducible secretion and translocation of therapeutic proteins based on the chemically regulated lumER and memberER systems. **a** A modified proinsulin sequence was designed to feature FURs (purple lines) between B (blue)/C-peptide (green) and C/A-peptide (magenta). After removal of the retention signal, the proinsulin passes GA, where it is processed to the mature insulin by FURp. Media were harvested at specified time points and C-peptide ELISA was performed to measure the amount of processed insulin. **b** C-peptide concentration was measured in the cell media after the addition of rapamycin, as well as from non-stimulated (NS) cells. Secretion kinetics of the lumER-insulin system was compared to the kinetics of secreted insulin in an inducible transcription-activation system. The secretion was compared with cells, which were not stimulated with rapamycin. **c** IL10 concentration was measured in the cell media after the addition of rapamycin, as well as from NS cells. Values are the mean of three cell cultures \pm s.d. and are representative of two independent experiments. An unpaired two-tailed *t* test (after equal variance was assessed with the F test assuming normal data distribution) was used for the statistical comparison of the data. **d** Scheme for memberER CAR T translocation from ER to plasma membrane after proteolytic cleavage. **e** Secretion of hIL-2 as a result of activation of Jurkat cells expressing memberER CAR T by addition of Raji cells. Values are the mean of three (**e**) and four (**b**, **c**) cell cultures \pm s.d. and are representative of two (**b**) and three (**c**, **e**) independent experiments. An unpaired two-tailed *t* test with Welch's correction was used for statistical comparison of the data. Source data are provided as a Source Data file.

Here two orthogonal systems for the release of pre-synthesized proteins from the ER by the proteolytic removal of a C-terminal ER-retention signal were presented. Both the lumER and the memberER system are able to secrete proteins substantially faster than engineered systems, which rely on the transcriptional regulation of secretory proteins. Both systems described here offer a tunable, concentration-dependent release of proteins, which achieves the rate of secretion kinetics suitable for several faster-acting biological processes. We demonstrated the use of a chemically regulated TEVp, as well as the activity of an additional highly specific and orthogonal viral protease, SbmVp, resident in the ER lumen. The lumER system proved to be the faster of the two, leading to protein secretion approximately 45 min after stimulation. This difference could be due to the requirement for processing by a single protease in lumER, whereas the memberER system requires additional processing by the FURp. Additionally, the substrate and split protease concentration might be higher in the ER, compared to the cytosolic protease. The CPS trafficking kinetics and capacity itself poses a limit on the speed of secretion as proteins can be transported inside the transport vesicles from ER to GA and further on to the plasma membrane at a certain maximal rate⁶¹, preventing the system to reach the kinetics of granule release in specialized cells. Inducible trafficking has been

previously achieved with biotin-based release to ER-resident hooks⁶² as well as light-triggered release⁶³, which however require fusion to the cargo protein and might be difficult to adapt for combinations of signals. An important feature of the platform reported here is that it relies on the removal of the retention signal by well defined, orthogonal and inducible proteases with high selectivity. This allows the systems to be incorporated into a variety of processing modules, which result in the activation or inactivation of an effector protease, thus allowing for precise control of protein secretion. As shown here, this processing can incorporate Boolean logic functions, and could potentially be expanded to feature other protein circuits¹⁶, feedback loops etc. Furthermore, inducibility of the input protease could be controlled by a variety of heterodimerization domains⁶⁴. This endows our system with a versatility not found in similar systems, which also rely on the accumulation of pre-synthesized proteins inside of ER, but retain the protein inside the ER in form of conditional protein aggregates³¹. Importantly the systems described here rely on monomeric proteins, avoiding protein aggregates, which eliminates the danger of the aggregated protein response.

Post-translational modifications of proteins, which occur in the CPS pathway may interfere with designed proteins and certain systems need to be optimized when translocated to the ER, as we

demonstrated for the PPVp for the lumER system. While certain modifications can restore protein activity (as demonstrated in the case of erTEVP³²), not all proteins could be readily transformed to function within the ER, presenting a challenge which needs to be addressed individually for each system. However, we presented several functional modules such as the erSbMVp and designed coiled-coil heterodimerization domains that could be combined into new functional circuits within the ER. On the other hand, certain post-translational processes can be used to the advantage of a designed system, such as the proteolytic cleavage by the GA-localized FURp, which we utilized for the release of proteins from the plasma membrane, as well as for the processing of the engineered proinsulin into insulin.

After our manuscript has been initially submitted another preprint describing a similar chemically regulated secretion system has been published by Vlahos et al.⁶⁵ The RELEASE system is analogous to our memberER system, uses similar split proteases as described by us here and before¹⁵ and exhibits many similar features, such as information processing and secretion of therapeutically relevant proteins. Its kinetics is likely similar to the kinetics described here.

In summary, the presented platform of protein secretion regulation based on modulation of protein recycling to the ER through cleavage of the retention signal present several advantages as a modular and scalable regulatory system that could be used in mammalian cells and likely in eukaryotic cells in general.

Methods

Plasmid construction. Plasmids were constructed using the standard procedures of molecular cloning or Gibson assembly. The amino acid sequences of all constructs are provided in Supplementary Table 1. All the protease coding sequences were codon optimized for expression in human cells, and the DNA was synthesized by IDT (PPVp, SbMVp, SuMMVp) or Life Technologies (TEVp). Split N- and C-fragments of proteases in fusion with CCs or dimerization partners FKBP/FRB and ABI/PYL1 were PCR amplified and inserted into the pcDNA3 vector. The FKBP and FRB domains were obtained from the pC4-RHE and pC4EN-F1 plasmids. ABI and PYL1 were obtained from pSLQ2816 pPB, as follows: CAG-PYL1-VPR-p2A-GID1-ABI-WPRE PGK-GAI-tagBFP-SpdCas9 (Addgene: 84261)³⁹. The GFP1-10 and GFP11x7 fragments were obtained from plasmids pcDNA3.1-GFP(1-10) (Addgene: 70219) and pACUH-GFP11x7-mCherry- α -tubulin (Addgene: 70218)⁴².

Mutations N23Q, C130S, and N171T in the wild type TEVp were made as in the design of erTEVP. SEAP was obtained from p_{PIR}ON-SEAP-pA which was kindly provided by Martin Fussenegger (Institute of Biotechnology, Swiss Federal Institute of Technology, ETH Zürich). The constructs for logical processing used with the memberER system were described by Fink et al.¹⁵.

The nuclease-deficient Cas9 was obtained from pHR-SFFVdCas9-BFP-KRAB (dCas9; plasmid 46911, Addgene). The gRNA containing MS2 aptamer sequences (gRNA_2 ms2) was synthesized by Life Technologies, amplified with PCR and inserted into the plasmid p_{gRNA}-humanized. All gRNA target sites were designed as 7 or 10 copies of the binding sites, separated by hypervariable linkers and synthesized by Genewiz, similar as previously described by Lebar et al.⁶⁶ dCas9 was fused with the heterodimerization domain FKBP or ABI. The VPR activator sequence was adapted from the Addgene plasmid 63801 and synthesized by Genewiz. The transcription activator was fused with either FRB or PYL heterodimerization domains, respectively, to allow for activation of transcription by the addition of either rapamycin or ABA to the cell media. Detailed information on the sequences used in this study are presented in Supplementary Tables 1–3.

Cell culture, SEAP detection, and luciferase assay. HEK293T and Jurkat E6.1 cells were obtained from the ATCC culture collection.

The human embryonic kidney (HEK) 293T cell line was cultured in DMEM medium (Invitrogen) supplemented with 10% fetal bovine serum (FBS; BioWhittaker, Walkersville, MD, USA) at 37 °C in a 5% CO₂ environment. Following this, 2 × 10⁴ HEK293T cells per well were seeded in clear 96-well plates (CoStar, Corning). At a confluence of 50–70% cells were transfected with a mixture of DNA and PEI (8 μ l PEI/1,000 ng DNA; stock concentration 0.324 mg/ml, pH 7.5). Detailed information about the amounts of plasmids in each experiment is provided in Supplementary Table 4.

Rapamycin (Sigma-Aldrich) and abscisic acid (ABA, Sigma-Aldrich) were each dissolved in dimethyl sulfoxide (DMSO) at concentrations 1 mM and 50 mM, respectively. Forty-eight hours after the transfection, cells were stimulated with rapamycin and/or ABA at a final concentration of 1.5 μ M and 50 μ M, respectively. At different time points after induction, media was harvested, centrifuged at 1200 × g

for 5 min to remove any leftover floating cells and transferred to a clear 96-well plate for SEAP detection or a white 96-well plate (CoStar, Corning) for luciferase assay. The remaining cells were harvested and lysed with 30 μ l of 1× passive lysis buffer (Promega).

To measure the time it takes for the complete secretion of the pre-synthesized and ER-localized protein, HEK293T cells (5 × 10⁵ to 7 × 10⁵) were seeded in six-well plates (Techno Plastic Products) and transfected the next day. 48 h after transfection cell media was changed and Eeyarestatin I (E1286) was added to a final concentration of 8 μ M. After 1 h cells were treated with rapamycin at a final concentration of 1.5 μ M and 10 μ l of cell media was harvested at specified time points.

SEAP was detected in the media and in the lysate with an alkaline phosphatase detection medium-powder QUANTI-Blue™ (InvivoGEN) as per the product's instructions. Briefly, 200 μ l of the resuspended QUANTI-Blue™ powder was added to 10–30 μ l of the harvested media or the cell lysate and incubated at 37 °C for 1–2 h. The absorbance of the media was measured at 630 nm with a Synergy Mx (BioTek) microplate reader. Normalized SEAP activity was calculated by dividing the set of values by the highest value in the experiment. In the secretion kinetics experiment the values for the memberER, lumER and transcription systems were normalized separately. Firefly luciferase and Gaussia luciferase activity were measured using a dual luciferase assay (Promega) and an Orion II microplate reader (Berthold Technologies). Luciferase activity presented as relative light units (RLU) was calculated by dividing each samples Gaussia luciferase activity, measured in the cell media, by the constitutive Firefly luciferase activity determined in the lysed cells from the same sample. Normalized Gaussia luciferase activity was calculated by dividing the set of values by the highest value in the experiment.

Jurkat cells were electroporated using the Neon Electroporation System (Life Technologies). Cells were washed with PBS and resuspended in R buffer at a density of 3 × 10⁷ cells per ml. 100 μ l cells were mixed with 15 μ g of plasmid DNA mixture (10 μ g CAR member with or without 5 μ g of TEVp; 10 μ g of conventional CAR was used as a control) and electroporated (1600 V, 3 pulses, 10 ms). Immediately after pulsing, cells were transferred to one well of a 12-well plate containing pre-warmed complete RPMI 1640 medium. The next day, 24 h post electroporation, cells were counted and seeded in 96 well plate with target Raji cells at a ratio of Effector (Jurkat-CAR T):Target (Raji)=5:1. Stimulation with target cells was terminated after 24 h by removal of media. Media was used for ELISA detection of interleukin-2 (hIL-2), produced as a result of Jurkat CAR T-cell activation.

memberER CAR T imaging. Twenty-four hours after electroporation cells were washed twice in buffer (2% BSA in PBS) before cell surface staining with fluorescent-labeled-antibody (anti-c-Myc 9B11 Alexa Fluor 647). Cells were resuspended in 100 μ l buffer containing antibody diluted 1:200 and incubated at 4 °C for 30 min. Cells were washed twice with PBS and imaged using a Leica TSC SP5 confocal microscope equipped with an HCX plan apo 63× (NA 1.4) oil-immersion objective. A 10-mW 633 nm HeNe laser was used for Alexa Fluor 647 excitation (emission between 650 and 750 nm). For acquisition, Leica LAS AF software was used and for image processing, LAS AF and ImageJ software were used.

Imaging and in situ monitoring of protein trafficking. 5 × 10⁴ HEK293-T cells per well were seeded in an 8-well chamber slide (ibidi). At a confluence of 50–70% cells were transfected with a mixture of DNA and PEI (8 μ l PEI/1,000 ng DNA). Detailed information about the amounts of plasmids in each experiment is provided in Supplementary Table 4. Forty-eight hours after transfection, HEPES was added to a final concentration of 20 μ M. For experiments of monitoring inducible protein trafficking, cells were treated with rapamycin and/or ABA at a final concentration of 1.5 μ M and 50 μ M, respectively. Cells were imaged using a Leica TSC SP5 confocal microscope equipped with an HCX plan apo 963 (NA 1.4) oil-immersion objective. During imaging, the cells were kept at 37 °C. For acquisition, Leica LAS AF software was used and for image processing LAS AF and ImageJ software were used.

Image analysis. To analyze organelle colocalization, cells were transfected with memberER and lumER constructs, which featured a TagRFP fluorescent protein, and co-transfected with fluorescent proteins, which localize to ER⁶⁷, GA⁶⁸ or plasma membrane⁶⁹. For acquisition, Leica LAS AF software was used. For plasma membrane colocalization, the membrane-localized area was carefully selected based on the co-transfected reporter signal. Colocalization of the TagRFP signal with a second, organelle localized fluorescent signal, was measured by calculating Pearson's correlation coefficient using ImageJ (Analyze tab/Colocalization/Colocalization Test).

Monitoring insulin, IL10 and hIL2 secretion with ELISA. Recombinant human proinsulin was designed according to Hay and Docherty²⁸ to allow for the secretion of the peptide through the conventional protein secretion pathway. The proinsulin sequence featured a furin protease cleavage site between B:C and C:A peptides, to allow for the processing to insulin inside of the GA. A TEV protease cleavage site and KDEL retention signal was fused to the C-terminal end of the

recombinant insulin. Similarly, a TEV protease cleavage site and KDEL retention signal were fused to the C-terminal end of human IL10. 10^5 HEK293T cells per well were seeded in clear 24-well plates (CoStar, Corning). At a confluence of 50–70% cells were transfected with a mixture of DNA and PEI (8 μ l PEI/1,000 ng DNA). Detailed information about the amounts of plasmids in each experiment is provided in Supplementary Table 4. Forty-eight hours after the transfection, cell media was removed and supplemented with fresh media. After 1 h, cells were stimulated with rapamycin at a final concentration of 1.5 μ M and media was harvested at specific time points after stimulation. The media was centrifuged for 5 min at 1200 \times g to remove any floating cells and 100 μ l media was transferred to a clear 96-well plate. Human insulin levels secreted from HEK293T cells were quantified using an Ultrasensitive C-peptide ELISA kit (Merckodia, cat. no. 10-1141-01) and the concentration was calculated from the standard curve based on the supplied calibrators. Human IL10 was quantified using The Human Interleukin 10 (IL-10) Uncoated ELISA Kit (Invitrogen, cat. no. 88-7106-88). Secreted human IL-2 was detected in cell media after cocultivation of Jurkat CAR T cells with Raji cell using The Human Interleukin 2 (IL-2) Uncoated ELISA Kit (Invitrogen, cat. no. 88-7025-77) according to manufacturer's protocol.

Transcriptional regulation of protein secretion. To compare the secretion kinetics of our post-translational modification-based system with secretion systems based on inducing gene expression, we cloned our reporter proteins SEAP and Gluc, as well as recombinant insulin under a minimal promoter, which featured 7 repeats of target binding sites [b]^{66,70}. Cells were seeded and transfected at a confluence of 50–70% cells with the plasmid, carrying the desired reporter protein, as well as plasmids coding for dCas9-FKBP, FRB-VPR and gRNA in the case of a rapamycin inducible system or dCas9-ABI, PYL-VPR and gRNA in the case of an ABA-inducible system. Detailed information about the amounts of plasmids in each experiment is provided in Supplementary Table 4. At determined time points, the media was harvested and the reporter activity was measured or protein concentration was determined accordingly.

The human preproinsulin, modified to feature FURs between B:C and C:A peptides, was cloned under a minimal promoter, which featured 10 repeats of gRNA target binding sites [ab]. pMin_insulin was used in combination with dCas9-FKBP and FRB-VPR to control the transcription of insulin by the addition of rapamycin.

Immunoblotting. HEK293T cells (5×10^5 to 7×10^5) were seeded in six-well plates (Techno Plastic Products). The next day, at a confluence of 50–70%, the cells were transiently transfected with a mixture of DNA and PEI (8 μ l PEI/1,000 ng DNA). Detailed information on the amounts of plasmids in each experiment is provided in Supplementary Table 4. At 48 h after transfection, the cells were washed with 1 mL PBS and lysed in 100 μ l of lysis buffer (40 mM Tris-HCl, pH 8.0, 4 mM EDTA, 2% Triton X-100 and 274 mM NaCl) containing a cocktail of protease inhibitors (Roche). Cells were lysed for 20 min on ice and centrifuged for 15 min at 17,400 r.p.m. to remove cell debris. The total protein concentration in the supernatant was determined with BCA assays. Proteins from the supernatant were separated on 12% SDS-PAGE gels (120 V, 60 min) and transferred to a nitrocellulose membrane (350 mA, 90 min). Membrane blocking, antibody binding, and membrane washing were performed with an iBind Flex Western device (Thermo Fisher) according to the manufacturer's protocol. The primary antibodies were rabbit polyclonal anti-AU1 tag (Abcam ab3401; diluted 1:2,000). The secondary antibodies were HRP-conjugated goat anti-rabbit IgG (Abcam ab6721; diluted 1:3,000) and HRP-conjugated goat anti-mouse IgG (Santa Cruz, sc2005; diluted 1:3,000). The secondary antibodies were detected with ECL western blotting detection reagent (Super Signal West Femto; Thermo Fisher) according to the manufacturer's protocol.

cdNA synthesis and RT-PCR. HEK293T cells (10^5) were seeded in twenty-four-well plates. The next day, at a confluence of 50–70%, the cells were transiently transfected with a mixture of DNA and PEI (8 μ l PEI/1,000 ng DNA). Detailed information on the amounts of plasmids in each experiment is provided in Supplementary Table 4. 24 h after transfection, cells were treated with 500 nM Thapsigargin (Tg) to induce ER stress. After and additional 24 h total RNA was isolated using High Pure RNA Isolation Kit (Roche). RNA quantity and purity were measured on Nanodrop spectrophotometer (Thermo Fisher Scientific) and 1 μ g of RNA was used to generate cDNA using High-Capacity cDNA Reverse Transcription Kit (Applied Biosystems™, cat. no. 4368813). After synthesis of cDNA, we performed quantitative real-time PCR using LightCycler® 480 SYBR Green I Master reaction mix (Roche). Relative expression of the spliced variant of XBP1 gene (XBP1s) was determined using reverse transcription-quantitative polymerase chain reaction (RT-qPCR). The expression levels of the target gene were normalized with glyceraldehyde-3-phosphate dehydrogenase (GAPDH) (reference gene). The comparative CT method ($\Delta\Delta$ CT method) was used to determine differential gene expression between samples. The primers used for qPCR were: hXBP1s_for 5'-gagtcgccagcaggtg-3', hXBP1s_rev: 5'-ccgcca-gaatccatggg-3'⁷¹, GAPDH_for: 5'-tgcaccaccaactgcttagc-3', GAPDH_rev: 5'-ggcatg-gactgtgctcatgag-3'⁷².

ATP determination assay. Cell viability was measured with an ATP Determination Kit (Invitrogen™, cat. no. A22066). Cells were seeded on a 96 well plate. After 24 h, cells were transfected with PEI. To induce ER stress, cells were treated with 500 nM Thapsigargin. After 48 h, cells were lysed and ATP was determined according to the manufacturer's instructions. Firefly luciferase activity was measured using an Orion II microplate reader (Berthold Technologies) and normalized cell viability was calculated by dividing the measured luciferase activity with the luciferase activity of cells treated with DMSO.

Software and statistics. Graphs were prepared with GraphPad Prism 8 (<http://www.graphpad.com/>). GraphPad Prism 8 was also used for statistical purposes. Values are the means of at least three/four biological replicates \pm standard deviation (s.d.) and are representative of at least two independent experiments. An unpaired two-tailed *t* test (equal variance was assessed with the *F* test assuming normal data distribution), one-way analysis of variance (ANOVA), Tukey's comparison and Dunnett's comparison were used for the statistical comparison of the data.

Reporting summary. Further information on research design is available in the Nature Research Reporting Summary linked to this article.

Data availability

The authors declare that the data supporting the findings of this study are available in the paper and its supplementary information files. The raw data are available from the corresponding author upon reasonable request. Source data are provided with this paper.

Received: 19 December 2021; Accepted: 23 February 2022;

Published online:

References

1. Benham, A. M. Protein secretion and the endoplasmic reticulum. *Cold Spring Harb. Perspect. Biol.* **4**, a012872–a012872 (2012).
2. Viotti, C. ER to golgi-dependent protein secretion: the conventional pathway. *Methods Mol. Biol.* **1459**, 3–29 (2016).
3. Pena, R. T. et al. Relationship between quorum sensing and secretion systems. *Front. Microbiol.* **10**, 1100 (2019).
4. Bonin-Debs, A. L., Boche, I., Gille, H. & Brinkmann, U. Development of secreted proteins as biotherapeutic agents. *Expert Opin. Biol. Ther.* **4**, 551–558 (2004).
5. Cotzomi-Ortega, I., Aguilar-Alonso, P., Reyes-Leyva, J. & Maycotte, P. Autophagy and its role in protein secretion: Implications for cancer therapy. *Mediators Inflamm.* **2018**, 4231591 (2018).
6. Xie, M. et al. β -cell-mimetic designer cells provide closed-loop glycemic control. *Science* **354**, 1296–1301 (2016).
7. Tai, K., Quintino, L., Isaksson, C., Gussing, F. & Lundberg, C. Destabilizing domains mediate reversible transgene expression in the brain. *PLoS ONE* **7**, e46269 (2012).
8. Quintino, L. et al. Functional neuroprotection and efficient regulation of GDNF using destabilizing domains in a rodent model of Parkinson's disease. *Mol. Ther.* **21**, 2169–2180 (2013).
9. Quintino, L. et al. Destabilizing domains enable long-term and inert regulation of GDNF expression in the brain. *Mol. Ther. —Methods Clin. Dev.* **11**, 29–39 (2018).
10. Andrae, L. C. & Burrone, J. The role of spontaneous neurotransmission in synapse and circuit development. *J. Neurosci. Res.* **96**, 354–359 (2018).
11. Boland, B. B., Rhodes, C. J. & Grimsby, J. S. The dynamic plasticity of insulin production in β -cells. *Mol. Metab.* **6**, 958–973 (2017).
12. Hughes, H. & Stephens, D. J. Assembly, organization, and function of the COPII coat. *Histochem. Cell Biol.* **129**, 129–151 (2008).
13. Jensen, D. & Schekman, R. COPII-mediated vesicle formation at a glance. *J. Cell Sci.* **124**, 1–4 (2011).
14. Stornaiuolo, M. et al. KDEL and KKXX retrieval signals appended to the same reporter protein determine different trafficking between endoplasmic reticulum, intermediate compartment, and golgi complex. *Mol. Biol. Cell* **14**, 889–902 (2003).
15. Fink, T. et al. Design of fast proteolysis-based signaling and logic circuits in mammalian cells. *Nat. Chem. Biol.* **15**, 115–122 (2019).
16. Gao, X. J., Chong, L. S., Kim, M. S. & Elowitz, M. B. Programmable protein circuits in living cells. *Sci. (80-)* **361**, 1252–1258 (2018).
17. Szegezdi, E., Logue, S. E., Gorman, A. M. & Samali, A. Mediators of endoplasmic reticulum stress-induced apoptosis. *EMBO Rep.* **7**, 880–885 (2006).
18. Ma, W. & Goldberg, J. Rules for the recognition of dilysine retrieval motifs by coatomer. *EMBO J.* **32**, 926–937 (2013).
19. Zerangue, N. et al. Analysis of endoplasmic reticulum trafficking signals by combinatorial screening in mammalian cells. *Proc. Natl Acad. Sci. USA* **98**, 2431–2436 (2001).

20. Wilson, D. W., Lewis, M. J. & Pelham, H. R. B. pH-dependent binding of KDEL to its receptor in vitro. *J. Biol. Chem.* **268**, 7465–7468 (1993).
21. Wu, M. M. et al. Organelle pH studies using targeted avidin and fluorescein-biotin. *Chem. Biol.* **7**, 197–209 (2000).
22. Wu, M. M. et al. Mechanisms of pH regulation in the regulated secretory pathway. *J. Biol. Chem.* **276**, 33027–33035 (2001).
23. Bräuer, P. et al. Structural basis for pH-dependent retrieval of ER proteins from the Golgi by the KDEL receptor. *Science* **363**, 1103–1107 (2019).
24. Hoyos, V. et al. Engineering CD19-specific T lymphocytes with interleukin-15 and a suicide gene to enhance their anti-lymphoma/leukemia effects and safety. *Leukemia* **24**, 1160–1170 (2010).
25. Bass, J., Turck, C., Rouard, M. & Steiner, D. F. Furin-mediated processing in the early secretory pathway: Sequential cleavage and degradation of misfolded insulin receptors. *Proc. Natl Acad. Sci. USA* **97**, 11905–11909 (2000).
26. Gary, T. Furin at the cutting edge: from protein traffic to embryogenesis and disease. *Mol. Cell* **3**, 753–766 (2007).
27. Nishigori, T., Yanagita, M. & Takeuchi, T. Proinsulin cleaved by furin is processed to chromatographically mature insulin by carboxypeptidases in nonneuroendocrine cells. *Peptides* **17**, 789–796 (1996).
28. Hay, C. W. & Docherty, K. Enhanced expression of a furin-cleavable proinsulin. *J. Mol. Endocrinol.* **31**, 597–607 (2003).
29. Cao, J., Rehemtulla, A., Pavlaki, M., Kozarekar, P. & Chiarelli, C. Furin directly cleaves proMMP-2 in the trans-golgi network resulting in a nonfunctioning proteinase. *J. Biol. Chem.* **280**, 10974–10980 (2005).
30. Yi, L. et al. Engineering of TEV protease variants by yeast ER sequestration screening (YESS) of combinatorial libraries. *Proc. Natl Acad. Sci. USA* **110**, 7229–7234 (2013).
31. Rivera, V. M. et al. Regulation of protein secretion through controlled aggregation in the endoplasmic reticulum. *Science* **287**, 826–830 (2000).
32. Cesaratto, F., López-Requena, A., Burrone, O. R. & Petris, G. Engineered tobacco etch virus (TEV) protease active in the secretory pathway of mammalian cells. *J. Biotechnol.* **212**, 159–166 (2015).
33. Zheng, N. et al. Specific and efficient cleavage of fusion proteins by recombinant plux pox virus N1a protease. *Protein Expr. Purif.* **57**, 153–162 (2008).
34. Seo, J. K., Choi, H. S. & Kim, K. H. Engineering of soybean mosaic virus as a versatile tool for studying protein-protein interactions in soybean. *Sci. Rep.* **6**, 22436 (2016).
35. Fernandez-Rodriguez, J. & Voigt, C. A. Post-translational control of genetic circuits using Potyvirus proteases. *Nucleic Acids Res.* **44**, 6493–6502 (2016).
36. Merzlyak, E. M. et al. Bright monomeric red fluorescent protein with an extended fluorescence lifetime. *Nat. Methods* **4**, 555–557 (2007).
37. Schjoldager, K. T., Narimatsu, Y., Joshi, H. J. & Clausen, H. Global view of human protein glycosylation pathways and functions. *Nat. Rev. Mol. Cell Biol.* <https://doi.org/10.1038/s41580-020-00294-x> (2020).
38. Shikano, S. & Li, M. Membrane receptor trafficking: evidence of proximal and distal zones conferred by two independent endoplasmic reticulum localization signals. *Proc. Natl Acad. Sci.* **100**, 5783–5788 (2003).
39. Gao, Y. et al. Complex transcriptional modulation with orthogonal and inducible dCas9 regulators. *Nat. Methods* **13**, 1043–1049 (2016).
40. Liang, F. S., Ho, W. Q. & Crabtree, G. R. Engineering the ABA Plant stress pathway for regulation of induced proximity. *Sci. Signal.* **4**, rs2 (2011).
41. Cross, B. C. S. et al. Eeyarestatin I inhibits Sec61-mediated protein translocation at the endoplasmic reticulum. *J. Cell Sci.* **122**, 4393–4400 (2009).
42. Kamiyama, D. et al. Versatile protein tagging in cells with split fluorescent protein. *Nat. Commun.* **7**, 11046 (2016).
43. Sarwar, N. et al. Diabetes mellitus, fasting blood glucose concentration, and risk of vascular disease: a collaborative meta-analysis of 102 prospective studies. *Lancet* **375**, 2215–2222 (2010).
44. Komatsu, M., Takei, M., Ishii, H. & Sato, Y. Glucose-stimulated insulin secretion: a newer perspective. *J. Diabetes Investig.* **4**, 511–516 (2013).
45. Ogen-Shtern, N., Ben David, T. & Lederkremer, G. Z. Protein aggregation and ER stress. *Brain Res.* **1648**, 658–666 (2016).
46. Hunt, S. M. N., Tait, A. S., Gray, P. P. & Sleight, M. J. Processing of mutated human proinsulin to mature insulin in the non-endocrine cell line, CHO. *Cytotechnology* **21**, 279–288 (1996).
47. Kalwat, M. A. et al. Insulin promoter-driven gaussia luciferase-based insulin secretion biosensor assay for discovery of β -cell glucose-sensing pathways. *ACS Sens.* **1**, 1208–1212 (2016).
48. Kalwat, M. & Cobb, M. H. Measuring relative insulin secretion using a co-secreted luciferase surrogate. *J. Vis. Exp.* <https://doi.org/10.3791/59926> (2019).
49. Saraiva, M., Vieira, P. & O’Garra, A. Biology and therapeutic potential of interleukin-10. *J. Exp. Med.* **217**, e20190418 (2020).
50. Sato, T. et al. Engineered human tmpk/AZT as a novel enzyme/prodrug axis for suicide gene therapy. *Mol. Ther.* **15**, 962–970 (2007).
51. Sahillioglu, A. C., Toebes, M., Apriamashvili, G., Gomez, R. & Schumacher, T. N. Crash-it switch enables reversible and dose-dependent control of tcr and car t-cell function. *Cancer Immunol. Res.* **9**, 999–1007 (2021).
52. Hackett, T., Holloway, R., Holgate, S. T. & Warner, J. A. Release during acute inflammation in chronic obstructive pulmonary disease: an ex vivo study. *Respiratory Res.* **14**, 1–14 (2008).
53. Teeling, J. L., Cunningham, C., Newman, T. A. & Perry, V. H. The effect of non-steroidal anti-inflammatory agents on behavioural changes and cytokine production following systemic inflammation: Implications for a role of COX-1. *Brain. Behav. Immun.* **24**, 409–419 (2010).
54. Alcazar, O. & Buchwald, P. Concentration-dependency and time profile of insulin secretion: dynamic perfusion studies with human and murine islets. *Front. Endocrinol. (Lausanne)*. **10**, 680 (2019).
55. Guruswamy Damodaran, R., Poussard, A., Côté, B., Andersen, P. L. & Vermette, P. Insulin secretion kinetics from single islets reveals distinct subpopulations. *Biotechnol. Prog.* **34**, 1059–1068 (2018).
56. De Nicolao, G., Liberati, D. & Sartorio, A. Stimulated secretion of pituitary hormones in normal humans: a novel direct assessment from blood concentrations. *Ann. Biomed. Eng.* **28**, 1136–1145 (2000).
57. Hay, K. A. et al. Kinetics and biomarkers of severe cytokine release syndrome after CD19 chimeric antigen receptor-modified T-cell therapy. *Blood* **130**, 2295–2306 (2017).
58. Bhatt, T. et al. Sustained secretion of the antimicrobial peptide S100A7 is dependent on the downregulation of caspase-8. *Cell Rep.* **29**, 2546–2555 (2019). e4.
59. Guest, P. C. Biogenesis of the insulin secretory granule in health and disease. *Adv. Exp. Med. Biol.* **1134**, 17–32 (2019).
60. Krawczyk, K. et al. Electrogenetic cellular insulin release for real-time glycemic control in type 1 diabetic mice. *Science* **368**, 993–1001 (2020).
61. Hirschberg, K. et al. Kinetic analysis of secretory protein traffic and characterization of golgi to plasma membrane transport intermediates in living cells. *J. Cell Biol.* **143**, 1485–1503 (1998).
62. Boncompain, G. et al. Synchronization of secretory protein traffic in populations of cells. *Nat. Methods* **2012** 95 9, 493–498 (2012).
63. Chen, D., Gibson, E. S. & Kennedy, M. J. A light-triggered protein secretion system. *J. Cell Biol.* **201**, 631–640 (2013).
64. Lonžarič, J. et al. Design and applications of synthetic information processing circuits in mammalian cells. 1–34. <https://doi.org/10.1039/9781782622789-00001> (2017).
65. Vlahos, A. E. et al. Protease-controlled secretion and display of intercellular signals. *bioRxiv* <https://doi.org/10.1101/2021.10.18.464444> (2021).
66. Lebar, T., Lainšček, D., Merljak, E., Aupič, J. & Jerala, R. A tunable orthogonal coiled-coil interaction toolbox for engineering mammalian cells. *Nat. Chem. Biol.* **16**, 513–519 (2020).
67. Nilsen, N. J. et al. Cellular trafficking of lipoteichoic acid and Toll-like receptor 2 in relation to signaling: role of CD14 and CD36. *J. Leukoc. Biol.* **84**, 280–291 (2008).
68. Schaub, B. E., Berger, B., Berger, E. G. & Rohrer, J. Transition of galactosyltransferase 1 from Trans-golgi cisterna to the trans-golgi network is signal mediated. *Mol. Biol. Cell* **17**, 5153–5162 (2006).
69. Meško, M., Lebar, T., Dekleva, P., Jerala, R. & Benčina, M. Engineering and rewiring of a calcium-dependent signaling pathway. *ACS Synth. Biol.* **9**, 2055–2065 (2020).
70. Lebar, T. et al. A bistable genetic switch based on designable DNA-binding domains. *Nat. Commun.* **5**, 5007 (2014).
71. Konovalova, J. et al. Human-specific regulation of neurotrophic factors MANF and CDNF by microRNAs. *Int. J. Mol. Sci.* **22**, 9691 (2021).
72. Forstnerič, V. et al. CRISPRa-mediated FOXP3 gene upregulation in mammalian cells. *Cell Biosci.* **9**, 93 (2019).

Acknowledgements

The project was funded by Slovenian Research Agency (program P4-0176, projects J1-9173, Z4-2657, N4-0800) and European Research Council (ERC AdG MaCCChines 787115). This work was initially described as part of the Slovenian 2016 iGEM competition project (<http://2016.igem.org/Team:Slovenia/Demonstrate>) and we thank team members who are not listed as authors—M. Meško, T. Lebar, F. Lapenta, Ž. Strmšek, R. Krese, K. Leben, L. Magdevska, M. Gradišek, E. Merljak, K. Cerović, and Ž. Pušnik for their contribution in carrying out the initial experiments on which the rest of the work was based. Apart from the members of the 2016 iGEM team we would also like to thank B. Domevčič for helping with the experimental work. Lastly, we would also like to thank (Institute of Biotechnology, Swiss Federal Institute of Technology, ETH Zürich) for providing the plasmid P_{PIR}ON-SEAP-pA.

Author contributions

A.P., T.F., N.F., J.L. and R.J. designed the experiments. A.P., T.F., N.F. and J.L. analyzed the data. N.J., T.P. and S.R. performed the experiments. A.P. and M.B. performed single cell analysis and protein trafficking. R.J. conceived and supervised the study. A.P., T.F., and R.J. wrote the manuscript. All authors discussed and commented on manuscript.

Competing interests

The authors declare no competing interests.

Additional information

Supplementary information The online version contains supplementary material available at <https://doi.org/10.1038/s41467-022-28971-9>.

Correspondence and requests for materials should be addressed to Roman Jerala.

Peer review information *Nature Communications* thanks Barbara Di Ventura for their contribution to the peer review of this work.

Reprints and permission information is available at <http://www.nature.com/reprints>

Publisher's note Springer Nature remains neutral with regard to jurisdictional claims in published maps and institutional affiliations.



Open Access This article is licensed under a Creative Commons Attribution 4.0 International License, which permits use, sharing, adaptation, distribution and reproduction in any medium or format, as long as you give appropriate credit to the original author(s) and the source, provide a link to the Creative Commons license, and indicate if changes were made. The images or other third party material in this article are included in the article's Creative Commons license, unless indicated otherwise in a credit line to the material. If material is not included in the article's Creative Commons license and your intended use is not permitted by statutory regulation or exceeds the permitted use, you will need to obtain permission directly from the copyright holder. To view a copy of this license, visit <http://creativecommons.org/licenses/by/4.0/>.

© The Author(s) 2022